Paper Introdution:

Design and Performance Evaluation of the Vertex Detector of AGORA Based on Stitching MAPS Technology

Chengdong FU for VTX group

Design and Performance Evaluation of the Vertex Detector of AGORA Based on Stitching MAPS Technology

Tianyuan Zhang[a,1] **et al. (VTX group)**

[a] *Institute of High Energy Physics, Chinese Academy of Sciences, Beijing*

E-mail: tyzhang@ihep.ac.cn

Abstract: The identification of heavy quarks and τ leptons constitutes one of the core physics objectives of the Circular Electron Positron Collider(CEPC). To achieve high-precision reconstruction of decay vertices for short-lived particles, the vertex detector must possess the capability to precisely measure the trajectory parameters of charged particles near the interaction vertex. To this end, the CEPC vertex detector will employ two detector schemes. The baseline scheme will utilise advanced Monolithic Active Pixel Sensors(MAPS) technology to reduce detector mass per layer, with the first detector layer positioned 11 mm from the collision point to optimise reconstruction precision for collision parameters d_0 and z_0. This will be complemented by an alternative scheme employing conventional Taichu sensors to construct a dual-sensor detector, serving as a more robust and technologically mature option. Both schemes cover polar angles from 8.1° to 171.9°, fulfilling CEPC's requirement for full solid-angle coverage. Simulations conducted using the CEPC software (CEPCSW), assuming a single-point spatial resolution of 5 μm for the sensors, yield performance parameters for the vertex detector baseline scheme. These include material budget, detection efficiency, resolution of d_0 and z_0, and the impact of dead sensors on performance.

[1] Corresponding author.

Contents

New

Summary

Reorganize the text

Redraw the figure and add text

Add cases

(backup)

New

- Higgs, CEPC and reference detector in TDR

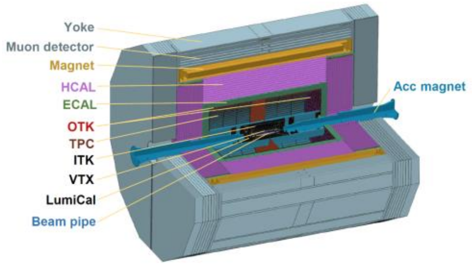

Figure 1: CEPC detector overview [1]

- Overview of TaiChuPix3 and stitching MAPS sensor
- Detail of layout of baseline VTX

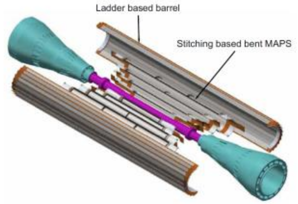

Figure 2: Overall layout of the CEPC vertex detector in the baseline configurations. The baseline design combines four inner stitching-MAPS layers with two outer planar CMOS layers. [1]

- Estimation of material budget
- Performance evaluation for cases
- Discuss on pixel size, vertex etc.

1 Introduction

Since the discovery of the Higgs boson by the ATLAS and CMS collaborations at CERN's Large Hadron Collider (LHC) in 2012, particle physics has entered a new era—the Standard Model (SM) has been completed, while simultaneously opening new avenues for exploring fundamental physics. Nevertheless, numerous unresolved questions persist regarding the nature of the Higgs boson, its role in the spontaneous breaking of electroweak symmetry, and its potential connections to physics beyond the Standard Model (BSM). To address these questions, China's particle physics community has proposed constructing the Circular Electron-Positron Collider (CEPC). Designed as a high-luminosity 'Higgs factory' operating at a centre-of-mass energy of 240 GeV, it will feature exceptionally high instantaneous luminosity and a pristine experimental environment. This will enable measurements of Higgs particle parameters—including mass, width, and couplings—with precision exceeding 1%. This will directly test whether the Higgs is a fundamental scalar or belongs to BSM frameworks such as supersymmetry, composite Higgs models, or dark matter interactions.

The CEPC adopts a two-phase strategy: Baseline: Operating in the 91–240 GeV range with a synchrotron radiation power of 30 MW, featuring a single collision point focused on

Similarities and Differences with TDR

- Detector layout

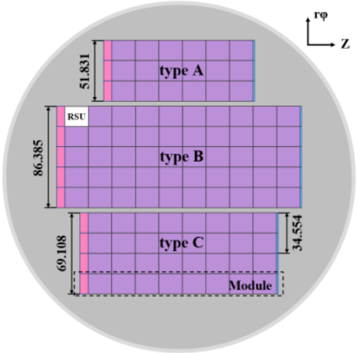

Figure 3: Sensor partition on a single wafer for the baseline stitching-MAPS design. Each region contains a different number of RSUs and modules to satisfy the geometrical requirements of individual detector layers. [1]

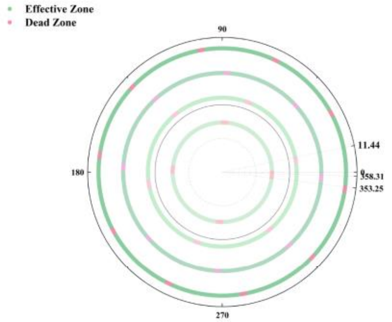

Schematic diagram of the Inner layer placement of the vertex detector stitching scheme.

Figure 5: Azimuthal arrangement of the first four vertex detector layers in the baseline design. A staggered placement is adopted to reduce the overlap of dead zones in the r-ϕ plane. [1]

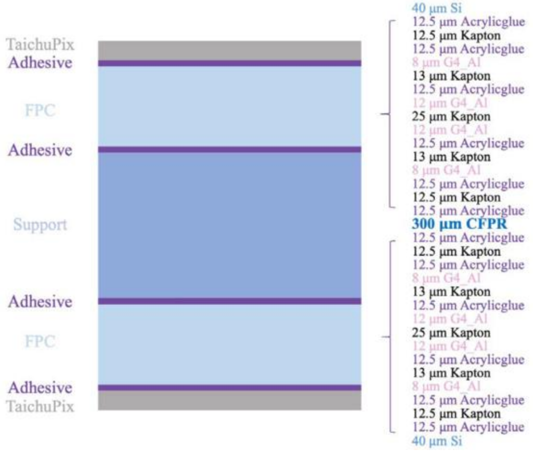

Table 1: Material layers onto CFRP support of planar Taichu layer

component	material	thickness [μm]	X/X0
TaichuPix	Si	40	0.0043
Adhesive	Acrylicglue	12.5	0.000358
FPC	Kapton	12.5	0.000383
	Acrylicglue	12.5	0.000358
	Al	8	0.00090
	Kapton	13	0.000398
	Acrylicglue	12.5	0.000358
	Al	12	0.00135
	Kapton	25	0.000766
	Al	12	0.00135
	Acrylicglue	12.5	0.000358
	Kapton	13	0.000398
	Al	8	0.00090
	Acrylicglue	12.5	0.000358
	Kapton	12.5	0.000383
Adhesive	Acrylicglue	12.5	0.000358

Table 4.3: Geometric configuration parameters. Radius and length, and material budget of the support structure for each layer of the VTX, as well as the arc length corresponding to CVTX and the height of ladder corresponding to PVTX.

CVTX/ PVTX X	radius mm	length mm	arc length mm	height mm	support thickness µm
CVTX 1	11.1	161.4	69.1	-	45
CVTX 2	16.6	242.2	103.7	-	32
CVTX 3	22.1	323.0	138.2	-	31
CVTX 4	27.6	403.8	172.8	-	29
PVTX 5	39.5	682.0	-	3.3	300
PVTX 6	47.9	682.0	-	3.3	300

new discussion on ideal stagger

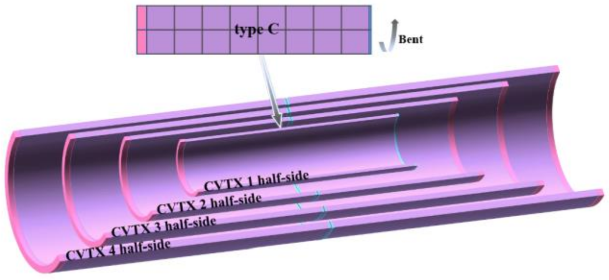

Figure 4: Schematic layout of the first four layers in the baseline vertex detector. The layers are formed by bent stitching sensors and assembled into semi-cylindrical structures around the beam pipe. [1]

A practical approach to determining the staggering angle involves calculating the product of the number of modules in the phi direction for two given layers, denoted as n_i and n_j. The maximum staggering angle $\Delta\phi$ required to offset the dead zones between these layers is given by

$$\Delta\phi = 360°/(n_i \times n_j). \quad (3.1)$$

Applying this formula, the theoretical staggering angles for layers 2 through 4 relative to the preceding layer are ±15°, ±7.5°, and ±4.5°. Furthermore, to prevent low-momentum tracks from consecutively traversing the dead zones of three adjacent layers, alternating staggering directions are implemented for successive layers. This ultimately results in a staggering scheme of 0°, 15°, 7.5°, and 12°.

Nevertheless, this configuration is optimal exclusively for high-momentum tracks. Under any given staggering scheme, tracks of a specific momentum will inevitably pass through two dead zones; thus, the primary design objective is to avoid scenarios where a track traverses three consecutive dead zones. In practice, this is further complicated by variations in dead zone dimensions. A performance comparison between this theoretically derived

Table 2: Geometric configuration parameters of baseline scheme.

layer	Nmodule	radius [mm]	Z length [mm]	rϕ width [mm]	support thickness [um]
CVTX1	4	11.1	161.4	69.1	45
CVTX2	12	16.6	242.2	103.7	32
CVTX3	16	22.1	323.0	138.2	31
CVTX4	20	27.6	403.8	172.8	29
PVTX5	24	39.5	682.0	17.3x24	300
PVTX5	24	47.9	682.0	17.3x24	300

Similarities and Differences with TDR

- Components and Material Budget
  - New description and add figure on azimuthal angle

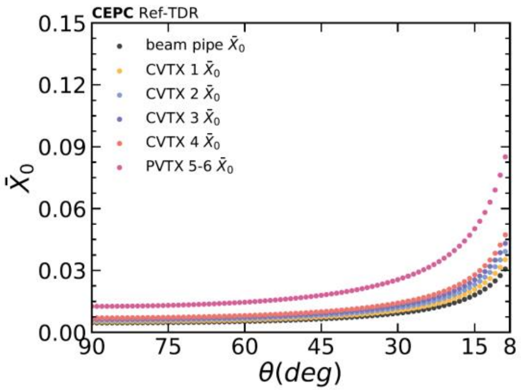

Figure 4.7: Average material budget $\bar{X}_0$ as a function of the polar angle θ, averaged over the full azimuthal angle ϕ, for each layer of the VTX and the beam pipe, is shown in a stacked plot. As θ decreases (i.e., moving toward the forward region), the effective path length through the detector increases, leading to a higher accumulated material budget. The four innermost curved MAPS layers (CVTX 1 ~ 4) exhibit significantly lower $\bar{X}_0$ values compared to the outer ladder-based layers (PVTX 5 ~ 6), reflecting the advantage of the low-mass inner design.

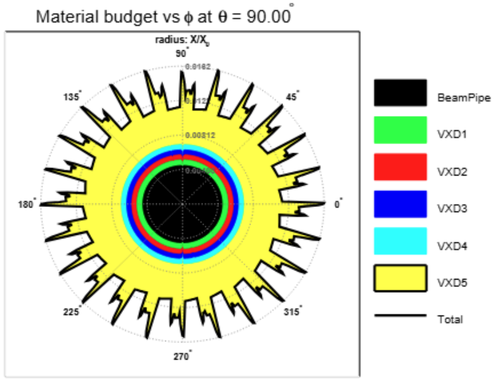

(a) Azimuthal angle at $\theta = 90°$.

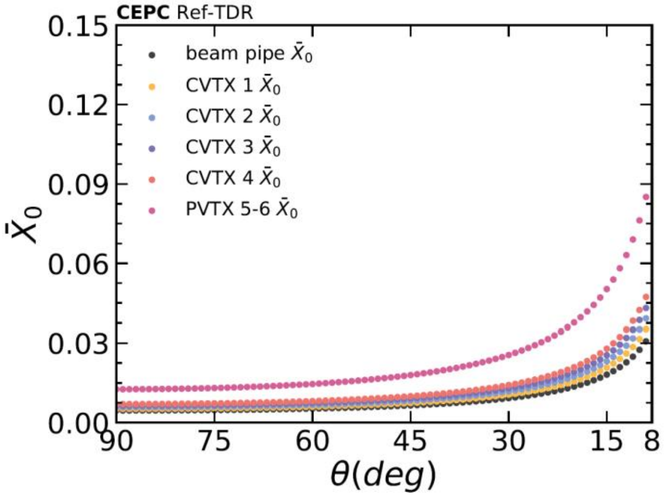

(b) Polar angle averaging in ϕ direction.

Figure 6: Material budget for the CEPC vertex detector baseline scheme. The contributions from the beam pipe and individual detector layers are shown separately. (a) Azimuthal angle at $\theta = 90°$. (b) Polar angle averaging in ϕ direction.

Similarities and Differences with TDR

- Performance

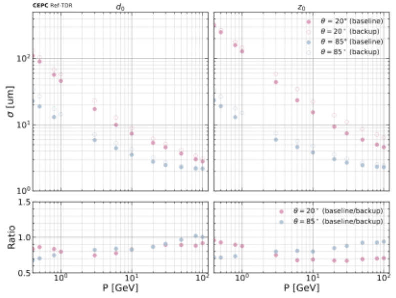

Figure 10: Impact-parameter resolution for the baseline and backup vertex detector schemes as a function of momentum at representative polar angles. The lower panels show the ratio of the baseline performance to the backup performance. [1]

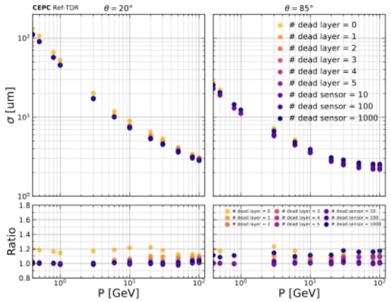

Figure 13: Degradation of impact-parameter resolution in the baseline scheme under dead-sensor scenarios. Results are shown for different numbers of randomly failed sensors and for the failure of an entire detector layer. [1]

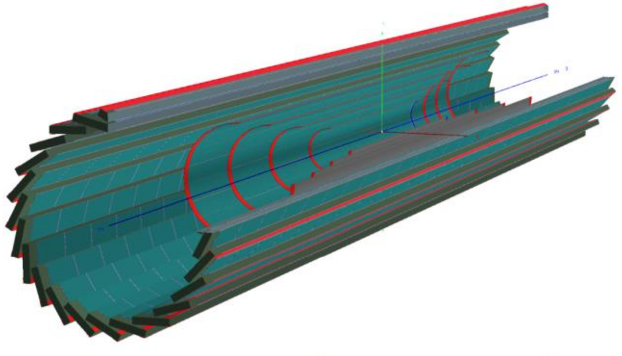

Figure 7: Visualization of the geometry of VTX described by DD4hep in CEPCSW.

- Add section Evaluation method: software overview

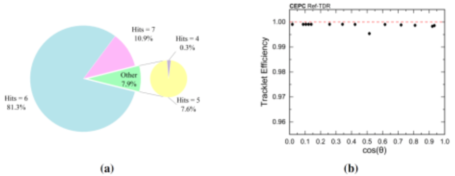

Figure 4.30: Tracking performance of the VTX. (a) Distribution of the number of hits per track for 10,000 charged Geantinos with p = 20 GeV and $\theta = 20°$. Most tracks have six hits (81.3%), while 10.9% of the tracks have seven hits, and the rest are distributed among four, five, or other configurations. (b) Tracklet efficiency as a function of $\cos\theta$ for charged Geantinos at 20 GeV, originating from the interaction point and passing through the VTX. The efficiency remains above 99.6% across all polar angles, demonstrating robust tracking performance.

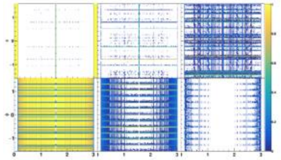

Figure 8: Distribution of the number of hits in the baseline vertex detector for charged geantino tracks. Most trajectories leave 5–7 hits in the six-layer detector.

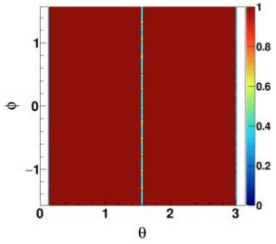

Figure 9: Tracklet efficiency of the baseline vertex detector as a function of polar angle and azimuthal angle. The efficiency remains high over the full angular coverage of the detector, and almost 100% at most of coverage.

different pixel size

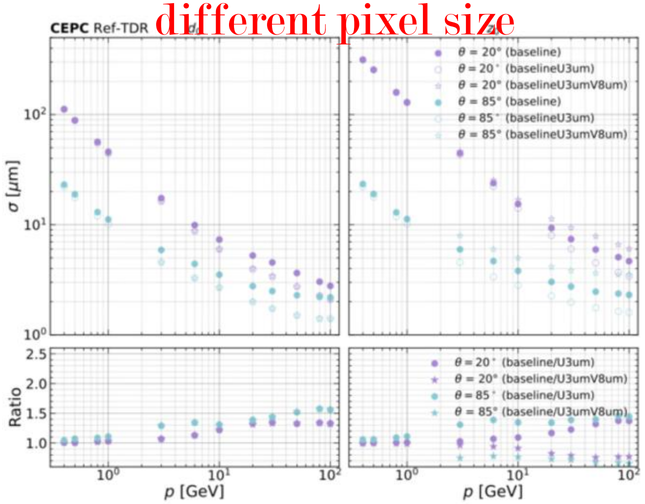

pixel size		spatial resolution
16μm	→	3μm
25μm	→	5μm
40μm	→	8μm

CVTX stagger

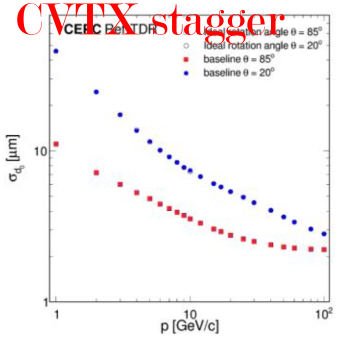

Figure 11: Resolution of d0 at different CVTX rotation angle.

Magnetic field

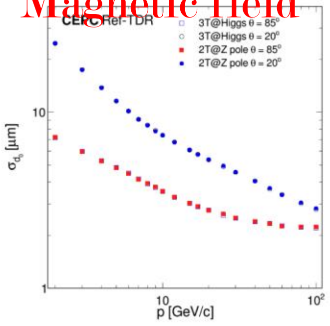

Figure 12: Resolution of d0 at different magnetic field.

Material change

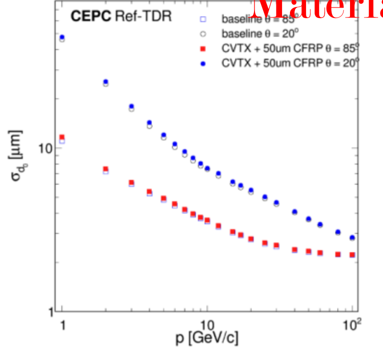

Figure 14: Resolution of d0 with thicken support for CVTX.

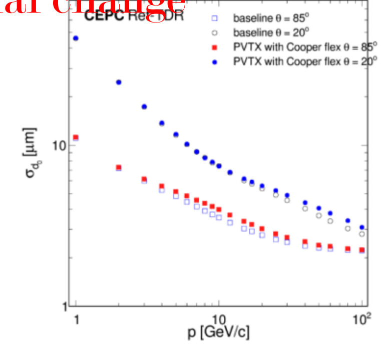

Figure 15: Resolution of d0 with cooper flex for PVTX.

Discussion and Conclusion

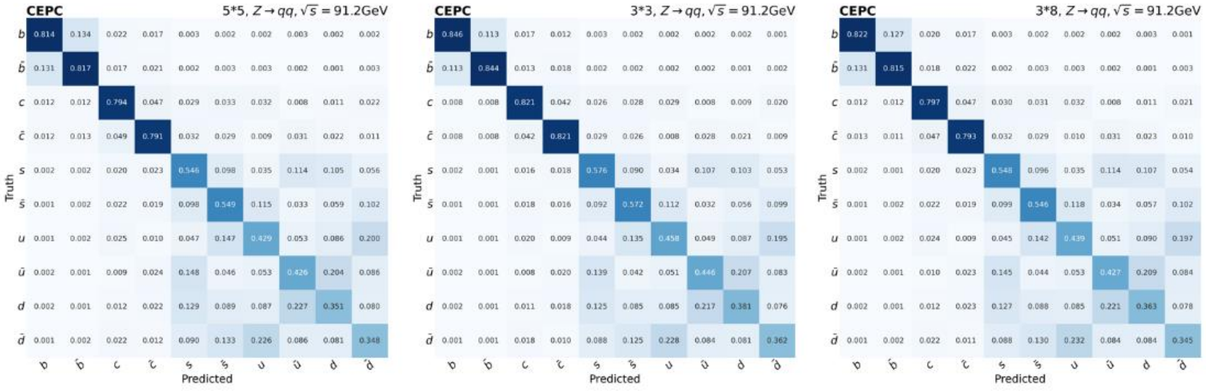

Figure 17: Flavor tag in different pixel size.

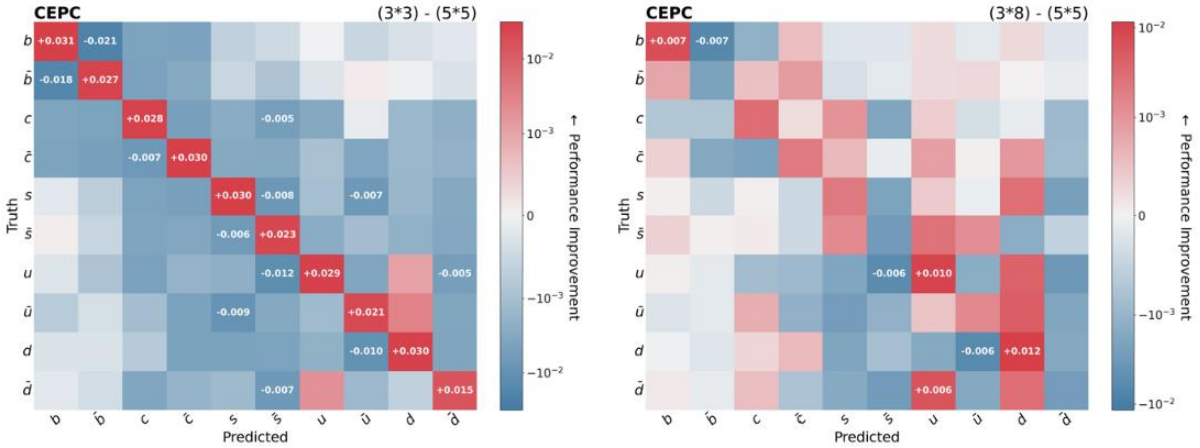

Figure 18: Improvement of flavor tag.

- The 16×16 μm² configuration achieves a 3% improvement across all flavors, representing a significant enhancement.
- Furthermore, the 16×40 μm² configuration performs comparably to the 25×25 μm² setup, avoiding the mixed performance observed between the 16×50 μm² and 25×25 μm² configurations.
- Overall, the performance hierarchy is 16×16 > 16×40 > 25×25.

TODO

- Figures
  - Merge partly
  - Redraw as style
- Text
  - Rewrite partly
  - Polish